SB³C2019
Summer Biomechanics, Bioengineering and Biotransport Conference
June 25 -28, Seven Springs, PA, USA

AN INTEGRATED OPTO-MECHANICAL SYSTEM FOR QUANTIFICATION OF DYNAMIC MICROSTRUCTURE AND MECHANICS OF HEART VALVE TISSUES

Samuel V. Jett (1), Zachary V. Schuermann (1), Arshid Mir (2), Harold M. Burkhart (3), and Chung-Hao Lee (1,4)

(1) Biomechanics and Biomaterials Design Laboratory
School of Aerospace and Mechanical Engineering
The University of Oklahoma
Norman, OK, USA

(2) Division of Pediatric Cardiology
Department of Pediatrics
University of Oklahoma Health Sciences Center
Oklahoma City, OK, USA

(3) Division of Cardiothoracic Surgery
Department of Surgery
University of Oklahoma Health Sciences Center
Oklahoma City, OK, USA

(4) Institute for Biomedical Engineering,
Science and Technology
The University of Oklahoma
Norman, OK, USA

INTRODUCTION

Many biomechanical diseases, such as heart valve stenosis, tendon tears, and arterial aneurysms, cause impairment in organ function via alterations and remodeling in tissue microstructure. Consequently, prior studies have examined the microstructure of healthy and diseased tissues [1]. Methodologies for microstructural analysis include histology, small angle light scattering (SALS), polarized light microscopy (PLM), and second-harmonic generation (SHG) imaging, among others. However, these techniques are incapable of capturing the *dynamic* nature of tissue microstructure and the collagen fibers therein. In collagenous tissues, such as the tendon and heart valves (HVs), the orientations and dispersion of the load-bearing collagen fibers dynamically adjust in response to mechanical loading [2]. In this study, we developed and validated a novel integrated system consisting of a biaxial tester and a polarized spatial frequency domain imaging (pSFDI) device to quantify load-driven changes to collagen microstructural architecture in tissues.

METHODS

Birefringent Microstructural Scattering Theory: Collagen fibers exhibit birefringence, i.e., a polarization-dependent refractive response. For a single fiber with coplanar polarization, the refractive index depends upon the fiber orientation (θ_f) relative to the polarization of the light (θ_p). The reflected light intensity (I) of the fiber under co-polarized illumination and capture is described by Eq. (1).

$$\mathrm{I} = a_0 + a_2 \cos\left(2\left(\theta_p - \theta_f\right)\right) + a_4 \cos\left(4\left(\theta_p - \theta_f\right)\right) \quad (1)$$

This birefringent relation between I, θ_f, and θ_p is further visualized in **Figure 1** with an example fiber angle of 90° and typical fitting Fourier series coefficients (a_0, a_2, a_4) as observed for collagen fibers.

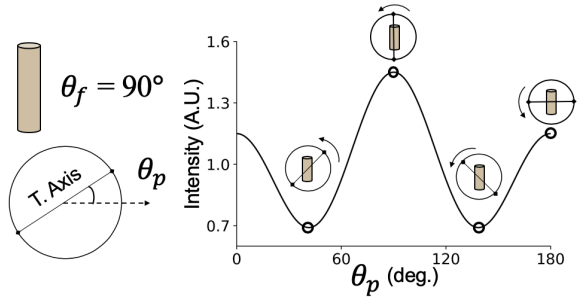

Figure 1: Schematic of the reflected intensity response of a collagen fiber at $\theta_f = 90°$ under co-polarized illumination and capture (T. Axis ~ Transmission axis of the polarizer).

This reflected intensity response holds for clusters of collagen fibers as well. In brief, the average orientation of a group of collagen fibers (θ) can be calculated as the θ_p where the reflected intensity is at its maximum. Additionally, the spread of the group of fibers can be represented via the degree of anisotropy (DOA) metric [3]:

$$\mathrm{DOA} = 1 - \left[\frac{a_0}{(a_0 + a_2 + a_4)}\right] \quad (2)$$

pSFDI System Theory: In pSFDI, a projector generates patterned images, according to spatial frequency domain imaging (SFDI) theory, and projects these images through a polarizer and onto a sample. The reflected light then passes through the same polarizer and is captured by a camera. To acquire the intensity response of the sample, the polarizer is incrementally rotated through 180° with an image captured at each increment. The pixelwise θ and DOA can be calculated by fitting Eq. (1) to the intensity response at each pixel and applying the fit coefficients to Eq. (2) (**Fig. 2a**).

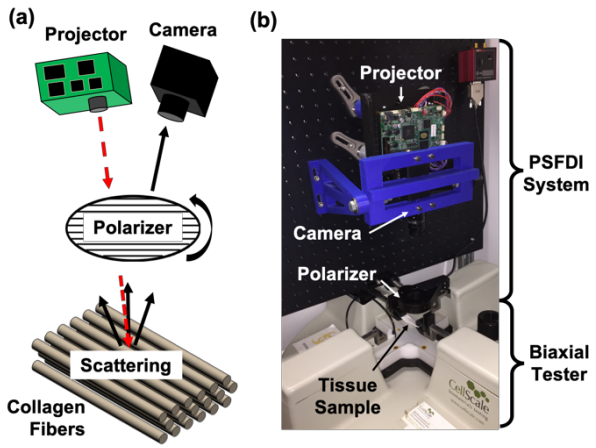

Figure 2: (a) Schematic showing the passage of light through the fundamental components of the pSFDI system, and (b) image of our integrated pSFDI and biaxial testing systems.

The Integrated System: Our group integrated a commercial biaxial tester (CellScale Biomaterials Testing, Canada) with a vertically-mounted pSFDI system to produce a combined opto-mechanical testing system (**Fig. 2b**). The testing sequence is controlled by in-house LabView programs and data/image analyses were performed in Python.

RESULTS

Tendon Tissue Testing: For validation, we performed uniaxial mechanical testing on a strip of bovine tendon with a 50° preferred fiber orientation, a width of 18 mm, and a thickness of 0.75 mm (**Fig. 3**).

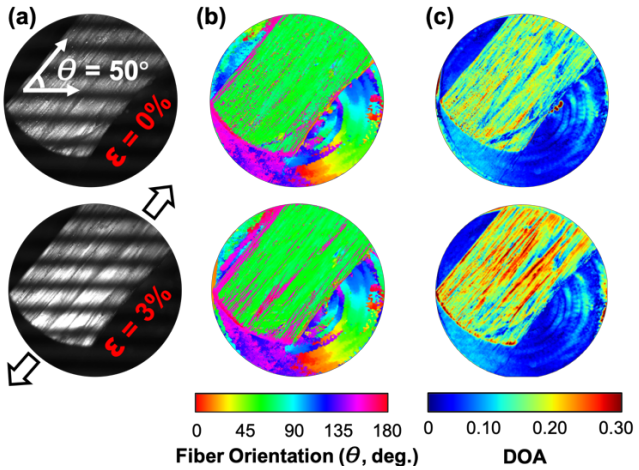

Figure 3: (a) Raw testing images, (b) θ predictions, and (c) DOA predictions for a tendon sample under 0% and 3% strains.

The θ prediction of 50° was accurate for both unloaded and loaded states, despite the appearance of some bands associated with 150° false predictions in the loaded tendon (**Fig. 3b**). On the other hand, the DOA predictions exhibited substantial load-dependency, with the domain-average DOA increasing from 0.145 for the unloaded tendon to 0.188 for the loaded tendon (**Fig. 3c**).

HV Leaflet Testing: We also used our system to examine the dynamic collagen microstructural architecture within a porcine mitral valve anterior leaflet (MVAL) with a thickness of 0.87 mm. We conducted a standard biaxial mechanical preconditioning protocol to restore the tissue's *in-vivo* behavior, then characterized the MVAL microstructure without loading (**Fig. 4c**) and under equibiaxial loading of 1.0 N (**Fig. 4d**).

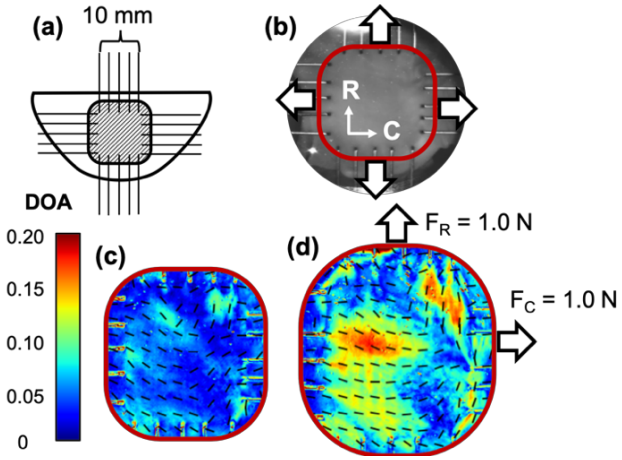

Figure 4: (a) Schematic of the MVAL testing region, (b) image of the mounted MVAL with directions marked (R: radial, C: circumferential). Predicted θ (dashed lines) and DOA: (c) without loads and (d) under an equibiaxial load of 1.0 N.

The fiber orientation predictions showed a strong bias toward the circumferential tissue direction but minor load-dependency, with domain-averaged θ of 177.1° prior to loading and 176.4° after loading. This bias manifested in the non-uniform dilation of the loaded tissue, with stretch of 29.7% in the radial direction but only 18.6% in the circumferential direction. In constrast to θ, the DOA showed a substantial response to external loads, with domain-averaged DOA increasing from 0.045 to 0.085 with applied loading. We also found subtle spatial variance in both the fiber orientation and DOA predictions.

DISCUSSION

The highly-uniform collagen orientation predicted in bovine tendon agrees with the known longitudinal fiber architecture. The increase in DOA we observed in the loaded tendon confirms intuition and suggests potential uncrimping of the collagen fibers with applied loads. For the HV leaflet tissue, our findings suggested that the loaded fibers: (i) are predominantly oriented in the circumferential direction and (ii) exhibit substantial spatial heterogeneity are supported by a mechanical study that found spatial differences and an increased circumferential stiffness in the MVAL mechanical response [4]. Although our study is the first to examine the fiber architectural changes in the full HV leaflet under biaxial loading, a prior study utilized SHG imaging and found microstructural load-dependency in the superficial layer [5]. Our study provides richer information to establish that MVAL load-dependency extends through the leaflet thickness. The similarity of tendon and MVAL microstructural predictions from this study to prior results validated the systemic capacity and opens doors to new research explorations, including: (1) novel applications in structural constitutive modeling, (2) understanding of the impacts of connective tissue disease on microstructure dynamics, and (3) improved microstructural analysis of fibrous biomaterials and engineered tissues.

ACKNOWLEDGEMENTS

This work is supported by the American Heart Association Scientist Development Grant 16SDG27760143 (CHL).

REFERENCES

[1] Jeffery, A et al., *J Bone and Joint Surgery*, 73(5):795-801, 1991.
[2] Driessen, N.J. et al., *J Biomech Engr*, 127(2):329-336, 2005.
[3] Goth, W et al., *Opt. E. and Tissue Biomechanics III*, 9710, 2016.
[4] Laurence, D et al., *J Biomech*, 34:859-871, 2018.
[5] Alavi, S et al., *Amer. J of Phys-H and C,* 309(2):276-284, 2015.